MOLECULAR CANCER BIOLOGY

INTERNATIONAL JOURNAL of CANCER

Germline gain-of-function MMP11 variant results in an aggressive form of colorectal cancer

Lorena Martin-Morales[1,2,3] | Sara Manzano[2,4,5] | Maria Rodrigo-Faus[4] | Adrian Vicente-Barrueco[4,6] | Victor Lorca[1,2] | Gonzalo Núñez-Moreno[7,8] | Paloma Bragado[2,4] | Almudena Porras[2,4] | Trinidad Caldes[1,2] | Pilar Garre[1,2,9] | Alvaro Gutierrez-Uzquiza[2,4]

[1]Molecular Oncology Laboratory, Hospital Clínico San Carlos, Madrid, Spain

[2]Health Research Institute of the Hospital Clínico San Carlos (IdISSC), Madrid, Spain

[3]Laboratory of Cancer Stemness, GIGA-Institute, University of Liege, Liege, Belgium

[4]Department of Biochemistry and Molecular Biology, Facultad de Farmacia, Universidad Complutense de Madrid, Madrid, Spain

[5]Biodonostia Health Research Institute, San Sebastian/Donostia, Spain

[6]Center for Cooperative Research in Biosciences (CIC bioGUNE), Basque Research and Technology Alliance (BRTA), Bizkaia Technology Park, Derio, Spain

[7]Department of Genetics, Health Research Institute-Fundación Jiménez Díaz University Hospital, Universidad Autónoma de Madrid (IIS-FJD, UAM), Madrid, Spain

[8]Bioinformatics Unit, Health Research Institute-Fundación Jiménez Díaz University Hospital, Universidad Autónoma de Madrid (IIS-FJD, UAM), Madrid, Spain

[9]Clinical Analysis Service, Molecular Diagnostic Unit, IML, Hospital Clínico San Carlos, Madrid, Spain

Correspondence
Alvaro Gutierrez-Uzquiza, Universidad Complutense de Madrid-Health Research Institute of the Hospital Clínico San Carlos (IdISSC), Madrid, Spain.
Email: alguuz@ucm.es

Abstract

Matrix metalloproteinase-11 (MMP11) is an enzyme with proteolytic activity against matrix and nonmatrix proteins. Although most MMPs are secreted as inactive proenzymes and are later activated extracellularly, MMP11 is activated intracellularly by furin within the constitutive secretory pathway. It is a key factor in physiological tissue remodeling and its alteration may play an important role in the progression of epithelial malignancies and other diseases. TCGA colon and colorectal adenocarcinoma data showed that upregulation of *MMP11* expression correlates with tumorigenesis and malignancy. Here, we provide evidence that a germline variant in the *MMP11* gene (NM_005940: c.232C>T; p.(Pro78Ser)), identified by whole exome sequencing, can increase the tumorigenic properties of colorectal cancer (CRC) cells. P78S is located in the prodomain region, which is responsible for blocking MMP11's protease activity. This variant was detected in the proband and all the cancer-affected family

members analyzed, while it was not detected in healthy relatives. *In silico* analyses predict that P78S could have an impact on the activation of the enzyme. Furthermore, our *in vitro* analyses show that the expression of P78S in HCT116 cells increases tumor cell invasion and proliferation. In summary, our results show that this variant could modify the structure of the MMP11 prodomain, producing a premature or uncontrolled activation of the enzyme that may contribute to an early CRC onset in these patients. The study of this gene in other CRC cases will provide further information about its role in CRC development, which might improve patient treatment in the future.

KEYWORDS

colorectal cancer, familial colorectal cancer type X, matrix metalloproteinase 11, proline for serine exchange in the 78 amino acid position of a protein, whole exome sequencing

What's new?

Matrix metalloproteinases have a tremendous capacity to degrade extracellular matrix proteins. While their activity has been closely associated with the invasive nature of malignant solid tumors, including colorectal cancer, their role in the carcinogenesis of colorectal adenomas remains unclear. Here, the authors unveil an *MMP11* variant able to produce a premature or uncontrolled activation of the MMP11 enzyme that may contribute to early disease onset in colorectal cancer patients. The identification of this new variant may facilitate the earlier detection of new tumors as they develop or become malignant in colorectal cancer patients.

1 | INTRODUCTION

Colorectal cancer (CRC) is the third most common cancer and the second leading cancer-related cause of death worldwide (all sexes, data from WHO [www.who.int] and World Cancer Research Fund [www.wcrf.org]). Although most CRCs are considered sporadic, it is estimated that familial risk is involved in up to 30% of all cases.[1] However, not more than 5% to 6% are caused by known germline mutations in cancer-predisposing genes.[2] The most common form of inherited CRC is Hereditary Non-Polyposis Colorectal Cancer (HNPCC), a familial syndrome characterized by an increased susceptibility to CRC and other associated tumors as defined by the Amsterdam I and II clinical criteria.[3,4] An important fraction of HNPCC constitutes Lynch syndrome, which is caused by germline inactivating variants in the mismatch repair (MMR) genes and leads to tumors presenting microsatellite instability (MSI). However, almost half of the families that fulfill the Amsterdam criteria show microsatellite-stable, MMR-proficient tumors and have a still unknown genetic basis. Consequently, they have been designated familial colorectal cancer type X (FCCTX).[5] Although next-generation sequencing (NGS) has allowed the identification of new CRC predisposition genes,[6] most FCCTX cases remain unexplained. FCCTX comprises a heterogeneous group of families that presumably includes different genetic syndromes. These may involve high or moderate-penetrance variants in novel cancer-predisposing genes, but they could also result from the combination of low-penetrance variants in different genes.[7] Therefore, identifying the different molecular mechanisms implicated in FCCTX

tumorigenesis remains a challenge and a priority. Hence, in our study we conducted whole exome sequencing (WES) to look for germline genetic alterations in a FCCTX family cohort that fulfilled the Amsterdam I/II criteria,[3,4] lacked MMR germline variants and presented MMR-proficient tumors. Although several candidate variants were identified in the family here presented, only the variant identified in the *MMP11* gene showed a perfect segregation with the disease.

Matrix metalloproteinase-11 (MMP11), also known as Stromelysin-3 (SL-3 or ST3), is a member of the matrix metalloproteinase (MMP) family or matrixins. The main biological function of this group of enzymes is the degradation of proteins from the extracellular matrix (ECM; eg, fibronectin, proteoglycans and collagen), for which they require the presence of metal ions such as Ca^{2+} or Zn^{2+}.[8-10] They are also known to control the shedding and releasing of biologically active chemokines, cytokines and growth factors,[11] being relevant in physiological processes such as morphogenesis, tissue remodeling and injury repair.[9,12] MMPs deregulation is strongly associated with pathologies such as arthritis,[13] brain disorders,[14] fibrosis,[15] heart failure[16] and cancer.[9,17,18] In this last disease, the role played by MMPs in the degradation of stromal connective tissue and basement membrane components make them key elements during tumor invasion and metastasis.[19] Although most MMPs are secreted and exert their function extracellularly, some of them, such as MMP1,[20] MMP2[21] and MMP11,[22,23] may be active inside the cell, modifying intracellular proteins.

Due to the great importance of these enzymes in the maintenance of homeostasis, their activity is regulated by several mechanisms, such as transcriptional regulation, mRNA processing, compartmentalization,

proteolytic processing or specific protein inhibitors (eg, tissue inhibitors of metalloproteinases or TIMPs).[9,24] The proenzyme regulatory mechanism is particularly important in this family of enzymes. They are produced as preproenzymes and processed during their translation to the plasma membrane. After this cleavage, MMPs remain in the form of inactive proenzymes that need to be activated.[12] The prodomain is formed by ~80 residues at the N-terminal region, containing a consensus conserved sequence, PRCXXPD, that forms the "cysteine-switch."[24] This domain interacts with the zinc-binding motif of the active center through three histidines that are coordinated with the cysteine by a Zn^{2+}, keeping the MMP in its inactive state. This prevents the interaction between a water molecule and the Zn^{2+}, which is essential for the catalytic activity of the protein.[12] Pro-MMPs are mainly activated by furin-mediated proteolysis at the recognition sequence RX[R/K]R, located in the C-terminal region of the propeptide.[24] Furin activity releases the propeptide, generating the active form of the MMP.[12] Particularly, MMP11 is intracellularly activated by furin, as well as by PACE4, in the trans-Golgi network,[22,25] being secreted as a 47 kDa active protease. Nonetheless, it can also be attached to the membrane or in intracellular compartments in its active form.[26] Multiple proteins degraded by MMP11 have been identified, including serpins such as A1AT, other protease inhibitors like A2M,[27] IGFBP-1,[27,28] β-casein (non-specific, weak activity)[27] and ERα (in vivo preliminary data).[29] MMP11 structure also includes four HPX (hemopexin-like) domains, which are common to other MMPs (eg, MMP1, MMP2, MMP3, MMP9 or MMP10), although their functions have not been fully determined. They may facilitate MMPs binding to other proteins, such as TIMPs or ECM components.

MMP11 has been found to be overexpressed in diverse types of cancer,[30] proving to be a critical factor in various malignant tumors such as lung cancer,[31,32] laryngeal cancer,[32] head and neck carcinoma,[33] gastric cancer,[34] breast cancer,[35,36] pancreatic cancer,[37] oral cancer[38] and CRC[39,40,41] through diverse clinico-pathological approaches. It is known that MMPs and TIMPs exert powerful effects on the local microenvironment during tumorigenesis and tumor progression. In addition, MMP11 has been evaluated as a predictive serum-based tumor marker in gastric, breast, colorectal and lung cancer.[42] Despite this, its potential as a CRC prognosis biomarker and its underlying molecular mechanism remains unclear. In the present study, we have investigated the MMP11-P78S variant and we provide evidence that it can be involved in the CRC carcinogenesis and increase the tumorigenic properties of CRC cells.

2 | MATERIALS AND METHODS

2.1 | Patient cohort

The studied family was recruited at the Genetic Counseling Unit of Hospital Clínico San Carlos (Madrid, Spain) and was part of a cohort of FCCTX families that fulfilled the Amsterdam I/II criteria,[3,4] lacked MMR germline variants and presented MMR-proficient tumors. Different family members were recruited for segregation studies, and formalin-fixed paraffin-embedded (FFPE) tumor blocks from cancer-affected relatives were obtained when available. Information on personal and family cancer history was obtained, and cancer diagnoses were confirmed by medical and pathology records. Healthy individuals recruited at the Blood Bank of Hospital Clínico San Carlos were used as controls, and FFPE tumor blocks from sporadic CRC patients were used as CRC controls.

2.2 | DNA and RNA extraction and quantification

Germline DNA and RNA were extracted from peripheral blood using the MagNA Pure Compact extractor system (Roche Diagnostics) and PAXgene Blood RNA Kit (PreAnalytiX), following the manufacturers' recommendations. Tumor DNA and RNA were extracted from 7-μm thick FFPE tissue sections, using the QIAamp DNA FFPE Tissue Kit and the RNeasy FFPE Kit (Qiagen), according to their protocols. A NanoDrop (Thermo Fisher Scientific) was used to assess DNA/RNA quantity and quality. However, for NGS purposes, DNA quality was also tested by agarose gel electrophoresis and its concentration was measured in a Qubit 3.0 Fluorometer (Life Technologies) and a 2100 Bioanalyzer (Agilent).

2.3 | Whole exome sequencing

WES was outsourced to *Sistemas Genómicos* (Valencia, Spain). The exome capture was performed using SureSelectXT Human All Exon V3 (51Mb, Agilent Technologies), and the library was sequenced on an Illumina HiSeq 2000 platform with paired-end reads of 101 bp and a ×50 average coverage depth. Reads were trimmed and aligned against the human reference genome version GRCh37/hg19 using the BWA software and processed by Picard-tools and SAMtools. The sequencing coverage and quality statistics for each sample are summarized in Table S1. Variant calling was performed using two different algorithms (VarScan and GATK), and the identified variants were annotated according to the recommendations of the HGVS.

2.4 | Variant filtering and prioritization

The identified variants were filtered for the selection of those: (a) shared by the cancer-affected family members; (b) carried in heterozygosis; (c) coding (frameshift, inframe, nonsense, missense) or splice region variants located in autosomes; (d) rare, with minor allele frequency (MAF) ≤0.01 in the general population according to GnomAD (gnomad.broadinstitute.org) and not present in three or more families and (e) predicted to be damaging by least four out of five in silico tools for missense variants (SIFT [sift.bii.a-star.edu.sg], PolyPhen [genetics.bwh.harvard.edu/pph2/], Condel [bbglab.irbbarcelona.org/fannsdb/], MutationTaster [mutationtaster.org] and PROVEAN [provean.jcvi.org]) and two out of two for inframe variants, or

predicted to alter splicing by the Human Splicing Finder (umd.be/HSF/) for splice region variants. Finally, filtered variants were prioritized based on the gene and variant location, thoroughly examining the literature and using UniProt (uniprot.org), OMIM (omim.org), Reactome (reactome.org), PathCards (pathcards.genecards.org), STRING (string-db.org), SMART (smart.embl-heidelberg.de) and cBioPortal's MutationMapper (cbioportal.org/mutation_mapper).

2.5 | Variant validation and segregation study

Candidate variants were validated by PCR followed by Sanger sequencing of the corresponding region of each gene (primers available upon request). The segregation was also assessed by Sanger sequencing in germline DNA from the available family members and tumor DNA from a deceased relative.

2.6 | Reverse transcription PCR and digital PCR

Reverse transcription PCR (RT-PCR) was performed using the PrimeScript RT Reagent Kit (Perfect Real Time, Takara, Clontech), following the kit's instructions. The absence of genomic DNA in cDNA samples was confirmed prior to their use by a PCR targeting exons 2 to 3 of *PALB2*. For the allele-specific expression assay, a custom TaqMan digital PCR (dPCR) was carried out taking advantage of the QuantStudio 3D Digital PCR System (Applied Biosystems) and according to the manufacturer's recommendations. Specific TaqMan probes were designed with the Custom TaqMan Assay Design Tool (Thermo Fisher Scientific) to recognize the P78S (FAM) or the wild-type (WT) allele (VIC). Duplicate samples of tumor cDNA from the carriers and sporadic CRC controls were assessed.

2.7 | Cell culture maintenance and reagents

HEK293T (RRID: CVCL_0063) and HCT116 (RRID: CVCL_0291) cells obtained from ATCC (Manassas, Virginia) were cultured in DMEM or McCoy's medium, respectively, supplemented with 10% fetal bovine serum (FBS) (Gibco, #10270106). All human cell lines have been authenticated using STR profiling within the last 3 years and were regularly tested to confirm that all experiments were performed with mycoplasma-free cells. Transfections were performed using Lipofectamine 2000 (1:3 ratio between DNA and transfection reagent), according to the manufacturer's protocol.

2.8 | Plasmid construction

A pTT3 plasmid containing the full-length *MMP11* cDNA fused to a *CD4* sequence and a bioHis tag (translated at the C-terminal end) was obtained from Addgene (#53408). The sequence of interest was cloned as a XbaI/NotI fragment into a pcDNA3.1 vector that included

two copies of the FLAG tag (DYKDDDDK), followed by two STREP tags (WSHPQFEK). The P78S variant was introduced by site-directed mutagenesis using the QuickChange mutagenesis kit (#200521, Agilent) and specific primers designed according to the cDNA sequence of the plasmid (forward: 5′-gcacgccgcatctactaggcctcaggctgc-3′ and reverse: 5′-gcagcctgaggcctagtagatgcggcgtgc-3′), following the manufacturer's instructions.

2.9 | Protein extraction and detection

Cells were lysed in RIPA buffer with protease and phosphatase inhibitors (PMSF 1 mM, aprotinin 10 μg/mL, leupeptin 10 μg/mL, Na_3VO_4 1 mM and NaF 20 mM). Protein concentration was measured by the BCA method (#10753505, #10341664, #10495944; Thermo Scientific), using a standard curve prepared with known concentrations of bovine serum albumin (BSA). Samples were sonicated for 2 minutes (20 seconds on and 20 seconds off cycles) and prepared in Laemmli buffer, followed by a 5-minute incubation at 95°C. Equal concentration of protein was adjusted with RIPA buffer. SDS-PAGE gels were transferred to PVDF membranes, blocked with 5% non-fat milk in tris-buffered saline 0.1% Tween (TBST) solution for 1 hour and then incubated with the specific primary antibodies (1:1000 dilution) (anti-FLAG: F3785, Sigma; anti-β-actin: #3700, CST; anti-MMP11: SN74-08, Invitrogen; anti-COL1A1: #72026, CST; anti-COL4A1: 55131-1-AP, Proteintech). Membranes were washed with TBST and incubated with anti-mouse (sc-2005, SCB) or anti-rabbit (sc-2004, SCB) HRP-conjugated secondary antibodies in 5% BSA TBST for 1 hour (1:5000 dilution). HRP luminescence was stimulated using the Clarity Western ECL Substrate (#170-5061, Bio-Rad) and detected with a VWR Chemi Imager Premium station. ImageJ was used for quantification.

2.10 | Immunoprecipitation and *in vitro* MMP11 activity assay

FLAG immunoprecipitation was conducted as described previously.[43] Pro-MMP11 activity was assessed in vitro as previously described.[44] Briefly, immunoprecipitates from cells transfected with FLAG-pro-MMP11 empty vector, WT or P78S constructs were incubated in reaction buffer[44] during 48 hours at 37°C either with 3 mg of collagen I (C3867-1VL, Sigma) or 3 mg of collagen IV (C6745, Sigma). Then, the cleavage of collagen chains was analyzed by Western blot using anti-collagen I (anti-COL1A1, #72026, CST) or anti-collagen IV (anti-COL4A1, 55 131-1-AP, Proteintech) antibodies.

2.11 | Invasion assay

The invasive capacity was analyzed using 8.0-μm pore transwells (Falcon, #353097) coated with two different matrices: Matrigel (250 μg/cm^2) (Corning, #356234) or collagen I (10 μg/cm^2) (Sigma

Aldrich, C3867). Cells (75 000) were seeded in the upper chamber in FBS-free medium and medium containing 10% FBS was added to the lower chamber to act as a chemoattractant. After 18 hours, invasion through the membrane was examined by cell fixation with paraformaldehyde (4%) for 20 minutes and crystal violet staining (0.2%) for 5 minutes. Extra stain was then removed, and cells were visualized with an Eclipse TE300 Nikon microscope coupled to a digital DS-U2 camera. ImageJ was used to count the cells that invaded through the matrix and the membrane.

2.12 | Viability assay

Cells (75 000) were seeded into 24-well plates in FBS-containing medium. After 24 hours, cells were fixed with paraformaldehyde (4%) for 20 minutes and stained with crystal violet (0.2%) for 5 minutes. Then, extra stain was removed, and cells were visualized with an Eclipse TE300 Nikon microscope coupled to a digital DS-U2 camera. ImageJ was used to count the cells.

2.13 | Protein modeling

Protein modeling was performed based on the sequence of WT MMP11 (UniProtKB-P24347) (UniProt 2019) and the P78S protein using the I-TASSER web server (https://zhanglab.ccmb.med.umich.edu/I-TASSER/).[45-47] Once the structural models were obtained in PDB format, the TM-Align structural alignment server (https://zhanglab.ccmb.med.umich.edu/TM-align/)[48] was used to superpose both structures to graphically visualize the differences. PyMOL 2.0 (Schrödinger, LLC) was used to visualize and render the structures in PDB format. To perform MMP11 alignments in different species and alignments of all human MMPs, we used M-Coffee (http://tcoffee.crg.cat/apps/tcoffee/do:mcoffee),[49,50] obtaining all the sequences from UniprotKB (UniProt 2019). To facilitate the visualization of the results and obtain figures, ESPript 3.0 (http://espript.ibcp.fr/ESPript/ESPript/)[51] and the CLUSTAL_ALN files obtained in M-Coffee were used.

2.14 | Statistical analysis

The results are expressed as the mean value ± SEM of at least three independent experiments. Statistical analyses were made by unpaired Student's t-test, ordinary one-way ANOVA or two-way ANOVA multiple comparisons test, depending on the experiment (P value ≤ 0.05 being considered significant: $P ≤ 0.05$ indicated as *, $P ≤ 0.01$ indicated as ** and $P ≤ 0.001$ indicated as ***). GraphPadPrism 8.1 was used for the representation of the results.

2.15 | TCGA COAD-READ expression analysis

RSEM-normalized RNA-seq and clinical data of TCGA COAD and READ patient cohorts were downloaded from the BROAD Institute FIREBROWSE repository (http://firebrowse.org/). Data was graphically represented and statistically analyzed using R statistical environment (R Core Team, 2020). Statistical analyses were conducted using the Mann-Whitney U test. The P values <.05 were considered significant: $P < .05$ indicated as *, $P < 0.001$ as **, $P < 0.0001$ as *** and $P < 0.00001$ as ****.

3 | RESULTS

3.1 | Clinical presentations and family history

The family subject of our study showed an autosomal dominant mode of CRC inheritance, fulfilling the Amsterdam I clinical criteria with three CRCs in two consecutive generations, the earliest diagnosed at the age of 40 (Figure 1A). In addition, there were two additional gastrointestinal cancers in the family (esophageal and duodenal), and two breast cancers in distant relatives (Figure 1A). All the CRC-affected members tested presented microsatellite-stable tumors with positive expression of the MMR genes and lacked germline mutations in any of the MMR genes (Figure 1A). On the other hand, the tumors from members III:1 and III:3 were screened for *KRAS* and *NRAS* mutations with a negative outcome. The stages at which the CRCs were diagnosed were II, IIIB-C and IV for members II:1, III:1 and III:3, respectively (Figure 1A).

3.2 | Identification of *MMP11* variant in CRC patients

The whole exome was sequenced in two cancer-affected members of the family, II:1 and III:1 (with CRC diagnosed at 67 and 48, respectively, Figure 1A). After the thorough filtering and subsequent prioritization of the variants detected, five candidate variants were selected: NM_001142676 (*CHID1*): c.3G>A; p.(Met1), NM_001367806 (*PYGO1*): c.1084T>C; p.(Ser362Pro), NM_005940 (*MMP11*): c.232C>T; p.(Pro78Ser), NM020731 (*AHRR*): c.680G>C; p.(Cys227Ser) and NM033120 (*NKD2*): c.431T>A; p.(Met144Lys). The segregation of these variants could be assessed in germline DNA of three healthy relatives (III:4, III:6 and III:7) and in tumor DNA of the deceased members III:2 and III:3. Our study demonstrated that the non-synonymous substitution in *MMP11* was the only candidate variant that segregated with the disease (Table S2).

NM_005940 (*MMP11*): c.232C>T; p.(Pro78Ser) was carried by family members II:1, III:1 and III:3, diagnosed with CRC, and III:2, diagnosed with esophageal cancer (EsC), while it was absent in the healthy relatives studied (Figure 1A). The c.232C>T mutation present in the *MMP11* sequence as shown in Figure 1B, is situated in the prodomain of the enzyme (shown in Figure 1C). It should be noticed that this is a very rare variant, with a MAF in the general population of 0.000884. In addition, it was predicted to be damaging by four in silico tools (SIFT: Damaging, score: 0.01; PROVEAN: Deleterious, score: −6.05; Mutation Taster: Disease causing, prob: 0.999995; PolyPhen-2: Possibly damaging, score: 0.914). On the other hand, the differential

ID	Sex	Tumor	Dx Age	CRC location	Diff	CRC stage (TNM)	MSI	MMR IHC	MMR mut	KRAS, NRAS mut
II:1	F	CRC	67	Rectum	Unk	II	MSS	Positive	N/A	N/A
III:1	M	CRC	48	Rectum	Mod	IIIB-C (T4N1M0)	MSS	Positive	Negative	Negative
III:2	M	EsC	70	N/A	Unk	Unk	N/A	N/A	N/A	N/A
III:3	F	CRC	40	Left colon	Mod	IV	MSS	Positive	N/A	Negative
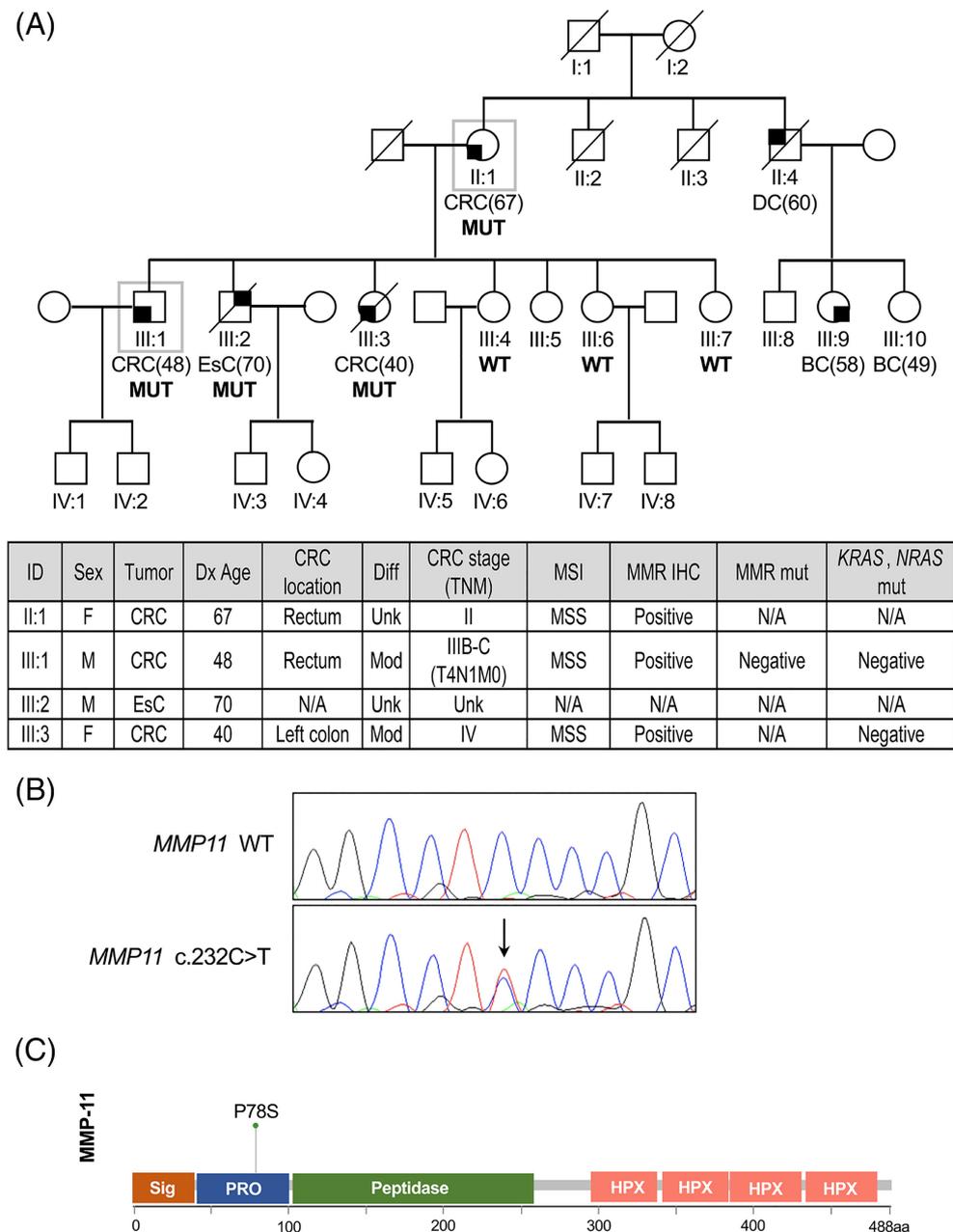
FIGURE 1 Germline *MMP11* variant identified in a FCCTX family. (A) Pedigree of the family where NM_005940 (*MMP11*): c.232C>T; p.(Pro78Ser) was identified. WES was done in members II:1 and III:1 (in a box), and the segregation was studied in III:2, III:3, III:4, III:6 and III:7. Four individuals were carriers (MUT), while another three were noncarriers (WT). Cancer-affected members are marked with a black corner; bottom left: CRC, top left: duodenal cancer (DC), top right: esophageal cancer (EsC), bottom right: breast cancer (BC). The age at diagnosis is shown between brackets. Different clinical and molecular features of the three CRCs are shown in the table. Diff, differentiation; Dx, diagnosis; IHC, immunohistochemistry; MMR mismatch repair; Mod, moderate; MSI, microsatellite instability; MSS, microsatellite stable; mut, mutation; N/A, not applicable; Unk, unknown. (B) Electropherogram of the WT and P78S sequence of *MMP11*. The arrow shows the location of the missense variant. (C) Lollipop plot showing the different protein domains of MMP11—Sig, signal peptide, mediating preproenzyme translocation; PRO, prodomain, which blocks MMP11 Zn-binding active site when inactive and its cleavage leads to protein activation; Peptidase, metallopeptidase domain which includes MMP11 active site; HPX, hemopexin-like domains—and the localization of the detected aminoacid substitution (P78S)

expression of the two alleles was assessed by digital PCR in tumor tissue from members III:1 and III:3. As observed in Figure 2, both tumors showed a positive expression of both the WT and mutant alleles and no overexpression of *MMP11-P78S* was detected. As expected, Sanger sequencing probed that all noncarrier controls only contained the WT allele. Given that *MMP11* had been previously reported to be involved in cancer aggressiveness, this variant was selected for further characterization.

FIGURE 2 Allele-specific expression of WT and P78S *MMP11*. (A) Digital PCR visualization of the allele-specific expression assay performed in the CRCs of family members III:1 and III:3, as well as in the CRC of a noncarrier used as a control. The FAM dye detects the P78S allele (in blue), while the VIC dye detects the WT allele (in red). (B) Quantification of the allele-specific expression obtained by digital PCR presented as Target/Total, where "Target" is the P78S *MMP11* allele. Data were collected from two independent experiments, and the error bars correspond to the confidence intervals
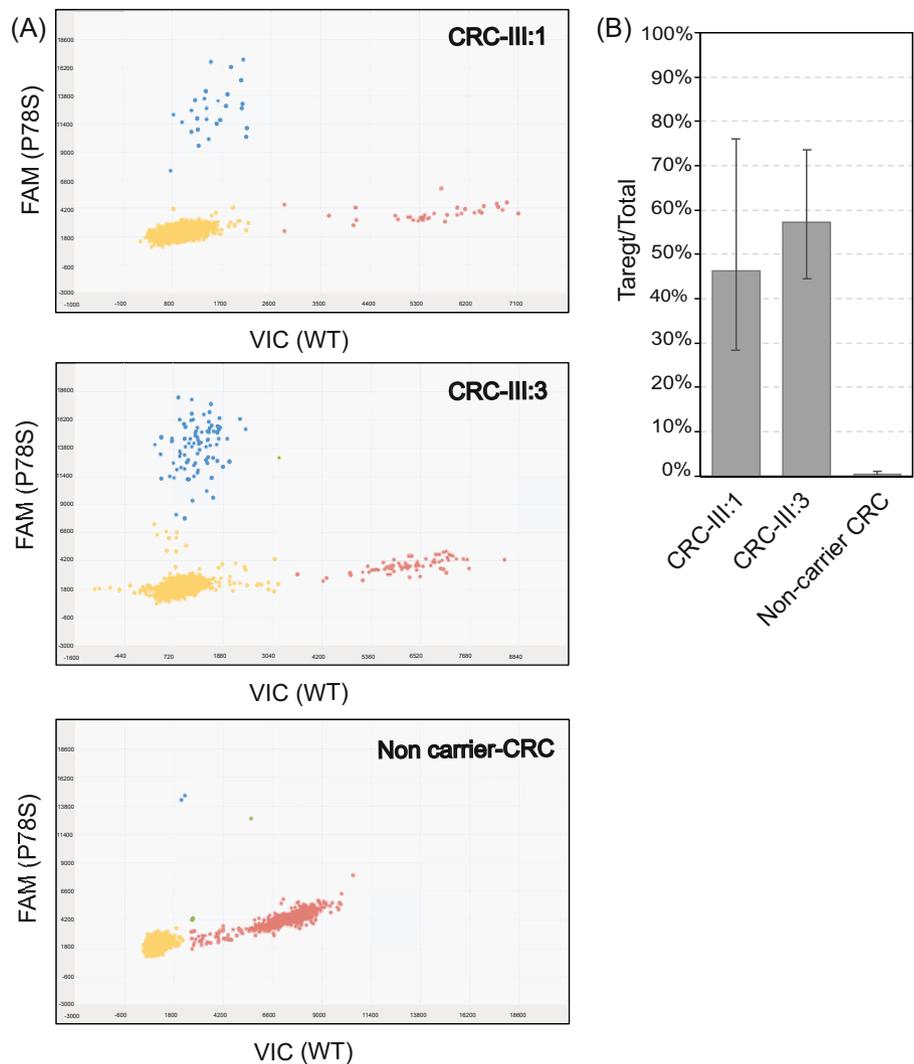
3.3 | *MMP11* expression analysis in TCGA CRC patients

To further explore the role of MMP11 in CRC malignancy, we analyzed the association of *MMP11* expression with overall survival, using the Kaplan-Meier method. Analyses using CANCERTOOL database[52] showed that patients with high *MMP11* expression exhibited a worse prognosis compared to those with low expression (Figure 3A).

A detailed analysis of RNA-seq samples from the TCGA CRC databases (COAD and READ) showed that *MMP11* levels were significantly up-regulated in tumor samples (red) compared to healthy tissue (gray) in both datasets (Figure 3B). Moreover, *MMP11* upregulation is associated with tumor progression and recurrence (Figure 3B-D), suggesting a putative role for MMP11 in CRC onset and development. On the other hand, we analyzed the potential impact of patient gender, age at diagnosis or the presence of *RAS* alterations, one of the hallmarks of CRC. However, we did not find any statistical effect of these parameters (Figure S1A-C).

3.4 | *In silico* effect of P78S on the MMP pseudosubstrate

An analysis of the amino acid sequence revealed that Pro78 is extremely conserved throughout evolution. Our analysis indicates that this residue is located at the end of the prodomain, at the beginning of an 8-amino acid sequence that is almost perfectly evolutionarily conserved, PRCGVPDV. In particular, the Pro78 residue is conserved in MMP11 sequence across the 24 species analyzed (Figure 4A). Furthermore, alignments of the 24 human MMPs "using MMP11 as a reference" identified four positions retained in all of them, namely Pro78, His179, Asp194 and Gly258 (Figure 4B). Interestingly, TPRCGVPDV sequence contains an unpaired cysteine that has been proposed to chelate with the prodomain, blocking MMP11 activity.[8,53] This reveals the importance of this region in the molecular regulation of the enzyme and suggests a potential role for Pro78. To gain further insight into the molecular alterations produced by the P78S variant on the activity of MMP11, we analyzed the structural repercussions of this modification in silico, predicted by a 3D model that was obtained and aligned. A standardized TM-Score of 0.9575 was
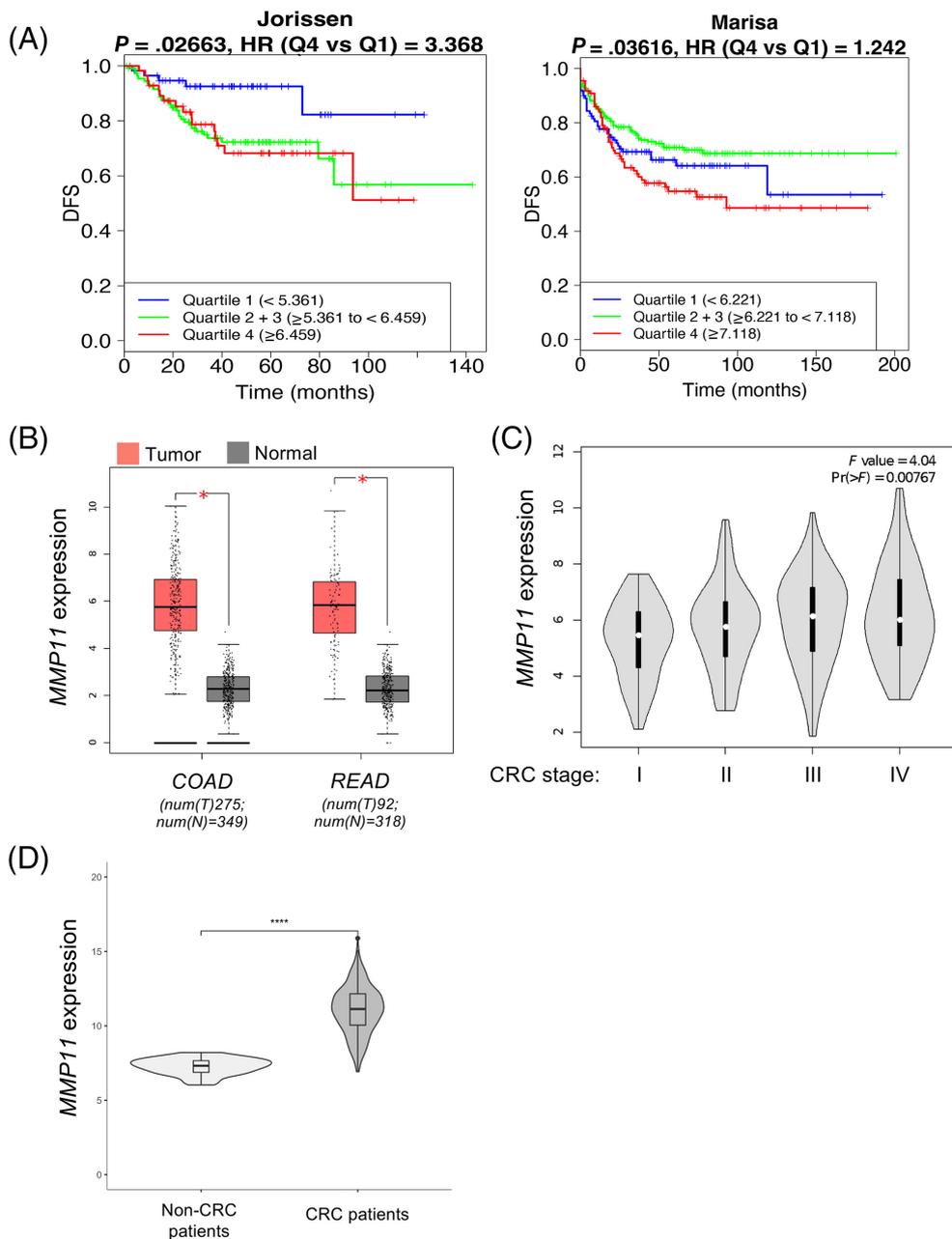
FIGURE 3 High levels of *MMP11* are associated with tumorigenesis and bad prognosis in CRC patients. (A) Kaplan-Meier curves showing the disease-free survival of CRC patients with high and low expression levels of *MMP11* (Data source: CANCERTOOL). (B) Box plots showing the difference in *MMP11* expression between normal (gray) and tumor (red) samples in READ and COAD patients (Data source: GEPIA). (C) Violin plots showing the difference in *MMP11* expression in CRC patients divided by stage (Data source: CANCERTOOL). (D) Box plots showing the difference in *MMP11* expression in normal tissue, primary or recurrent tumor in samples from CRC patients

obtained (where 1 means a perfect alignment of the structures), indicating that both proteins are very similar in terms of folding (Figures 4C and S2). However, the model predicted some changes in the pseudosubstrate region caused by the Pro78Ser substitution (Figure 4D). This pseudosubstrate acts as a molecular switch that keeps the protein in an inactive state by blocking the accessibility of the substrate to the active center. That is why we hypothesize that the P78S variant may have an impact reducing the ability of the pseudosubstrate to block the activity of the protein.

3.5 | MMP11P78S increases tumor cell invasion and proliferation

Previous reports have shown that overexpression of MMP11 variants affecting the pseudosubstrate had an impact on the activity of the protein.[53] To determine if the P78S variant affects the activity of the protein, constructs containing either the WT or the P78S version of *MMP11* were generated, using as a template a plasmid previously used to evaluate MMP11 activity in cellular models,[26] which was then cloned into a pcDNA3 vector containing a N-terminal α-Flag-STREP-tag and a C-terminal 6×-histidine (α-His) tag (Figure 5A). The expression of these constructs (WT and MMP11-P78S) was checked by western blot (WB) on HEK293T cells, showing that MMP11 was not detected in mock-transfected cells extracts, while several bands were identified after incubation with anti-α-FLAG or anti-MMP11 antibodies (Figure 5B). Incubation with anti-FLAG antibody showed a clear band (around 80 kDa) which corresponds to the pro-MMP11 form and a faint second band above this one, which could correspond to the pro-MMP11 with post-translational modifications and/or MMP11 complexes (90 kDa) (Figure 5B). WB quantifications indicate

FIGURE 4 Multiple sequence alignment and protein modeling. (A) Fragment of the Multiple Sequence Alignment (MSA) obtained from 24 sequences of different animal species to study the conservation of MMP11. The alignment was performed by M-Coffee and plotted by ESPript 3.0. Residues completely conserved in the studied species are highlighted in red. (B) Fragment of the MSA was performed to study residue conservation across all human MMPs. The alignment was performed by M-Coffee and plotted by ESPript 3.0. The Pro78 residue (MMP11 relative position) is highlighted in red. (C) Superposed I-Tasser protein structure model of WT and P78S MMP11, showing the different domains and residues of interest (see legend). (D) WT (in green) and P78S (in red) MMP11 renders with a magnification of the mutation region. P78 or S78 are shown in dark blue and the pseudosubstrate is shown in cyan. Greater exposure of the pseudosubstrate can be observed in the mutant model

that the 90 kDa band represents around 30% of the pro-MMP11 form (Table S3). Incubation with anti-MMP11 antibody showed three bands (90, 80 and 70 kDa). The first two correspond to the α-pro-MMP11 form overlapping α-FLAG bands (90 and 80 kDa), and the third one, only detected by the anti-MMP11 antibody, corresponds to the active form of MMP11 (70 kDa), in which the N-terminal FLAG tag has been
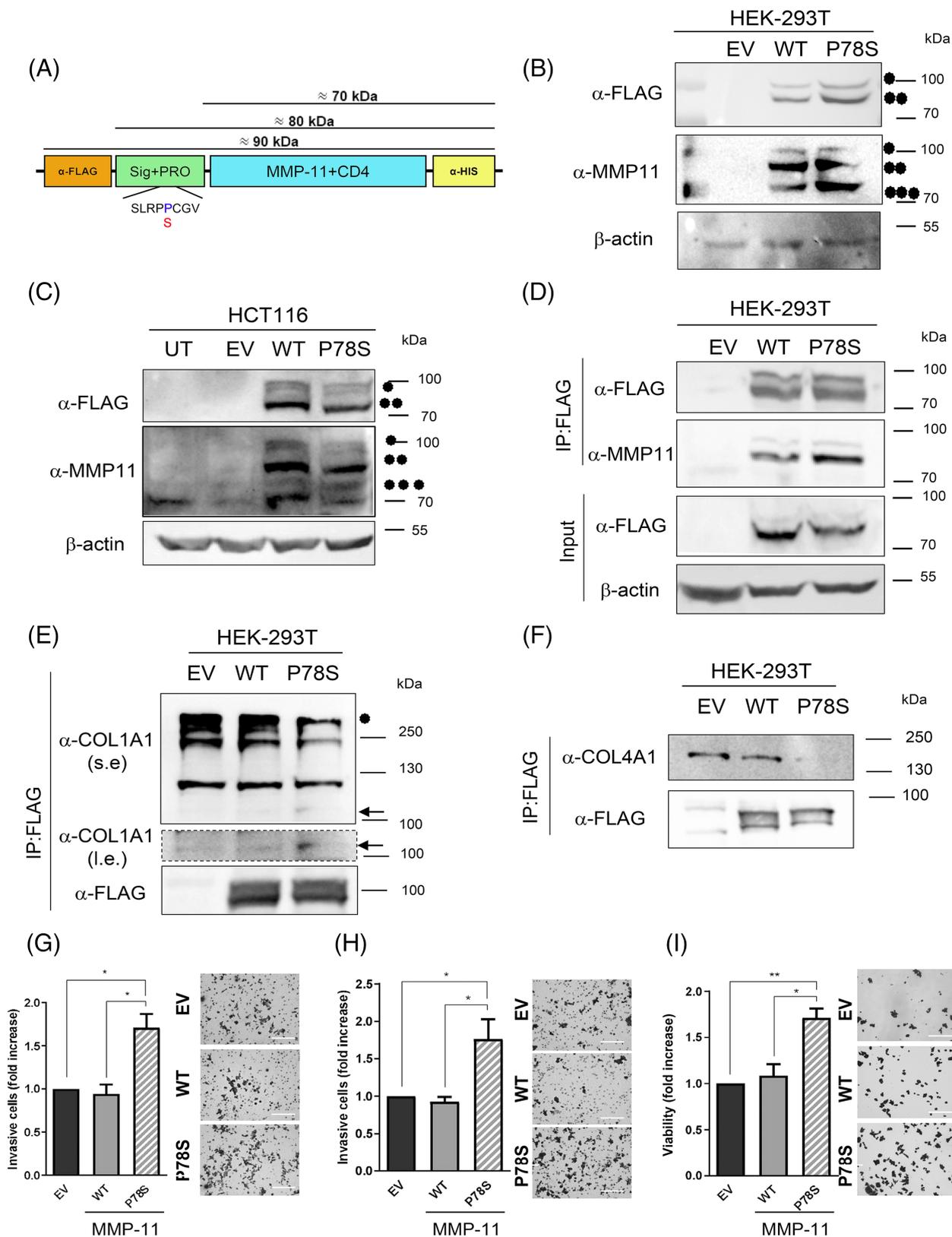
FIGURE 5 Legend on next page.

lost as a consequence of the proteolysis of the propeptide (Figure 5B). The active form represents around 30% to 50% of total amount of the MMP11 protein (Table S3).

To evaluate the functional consequences of MMP11-P78S, we used HCT116 cells, a well-established CRC *in vitro* model positive for MMP11.[51] In these cells, a WB analysis revealed a similar band pattern than in HEK293T cells showing 90, 80 and 70 kDa bands (Figure 5C). In addition, the WB analysis showed that transfection of P78S variant in HCT116 cells resulted in similar protein levels than WT version (Figure 5C), while no signal was detected on cells untransfected or transfected with the pCDNA3 empty vector (EV) used as control.

In addition, we performed immunoprecipitation (IP) analysis using anti-FLAG antibody against the N-terminal tag followed by detection with anti-MMP11 to clearly distinguish the pro-MMP11 from the cleaved/active forms (Figure 5D). MMP11 immunoprecipitation clearly showed two bands at 80 and 90 kDa. Both bands, positive for FLAG and MMP11 antibodies, would correspond to pro-MMP11 form. The upper band could correspond to post-translationally modified pro-MMP11. The 70 kDa band detected exclusively by MMP11 antibody was not present in FLAG immunoprecipitates (Figure 5D).

To study the effect of the mutation in the activity of the pro-MMP11 form of the enzyme, we transfected HEK293T cells and immunoprecipitated the pro-MMP11 form using antibodies against FLAG protein (Figure 5D). Then, we conducted an in vitro digestion of collagen I and IV (Figure 5E,F), incubating pro-MMP11 immunoprecipitates with these substrates in a reaction buffer previously described for other MMPs.[44] Western blot analysis showed reduced levels of collagen I and IV after incubation with the pro-MMP11 carrying the P78S mutation, while no detectable reduction was detected in immunoprecipitates from cells transfected with empty vector or pro-MMP11-WT (Table S3). These results suggest that pro-MMP11P78S has some enzymatic activity, even in the presence of the pro signal.

To assess aggressiveness, we analyzed the invasive skills of CRC cells using transwell assays. For that purpose, transwells were coated with either collagen I or Matrigel. We found that the invasion was increased in cells expressing the MMP11-P78S variant as compared to both cells expressing MMP11-WT or control cells, using FBS as a chemoattractant (Figure 5G,H). Moreover, this effect was independent of the type of matrix used for the assays. These results indicate that MMP11-P78S enhances the invasive capacity of CRC cells.

As previously mentioned, MMP11 is known to mediate aggressiveness in CRC and other tumors, such as lung and gastric cancer. Therefore, we decided to study the effect of the expression of MMP11-P78S on the viability of HCT116 cells. As shown in Figure 5I, we found that the number of cells was increased in cells expressing MMP11 P78S compared to both cells expressing MMP11-WT or the empty vector.

Our results suggest that expression of MMP11-P78S variant increases CRC cell invasion and viability possibly due to a premature activation of mutant MMP11, consistent with a gain of function effect.

4 | DISCUSSION

Matrix metalloproteinases are zinc-dependent endopeptidases with a tremendous capacity to degrade ECM proteins and whose activity has been closely associated with the invasive nature of malignant solid tumors, contributing to their high mortality and poor prognosis.[54] In particular, MMPs and their inhibitors, are especially important in the process of tumor invasion, progression and metastasis of CRC, one of the most common cancers worldwide. However, it has been proposed that, in addition to this function, these proteins may also play a role in the carcinogenesis from colorectal adenomas.[55]

In the present study, a germline variant in the *MMP11* gene (NM_005940 (*MMP11*): c.232C>T; p.Pro78Ser) was identified in a family with a significant history of CRC and other gastrointestinal tumors. The family belonged to a heterogeneous group of HNPCC families called Familial Colorectal Cancer Type X, whose genetic basis and molecular mechanisms of tumor predisposition remain unknown.[56] The variant was initially found by NGS in the two members that were screened and were later shown to co-segregate with all three CRCs of the family, as well as with esophageal cancer, while being absent in the healthy relatives. A digital PCR confirmed the expression of the variant in the available tumors, and subsequent studies based on the analysis of databases, protein sequences and structures, as well as in vitro

FIGURE 5 Overexpression of *MMP11*-P78S variant enhances pro-MMP11 activity leading to an increase in invasion and cell viability of CRC cells. (A) Representative scheme of *MMP11* cDNA, attached to *CD4*, in the pCDNA3.1 plasmid. The approximate molecular weights of full-length MMP11 + CD4 (that includes its prodomain [PRO]) and cleaved MMP11 + CD4 are denoted. The location of the FLAG (FLAG) and polyHis (HIS) tags is also indicated. Moreover, the Pro78 residue (which is replaced by a Ser in the MMP11-P78S variant) and its surrounding protein sequence are also shown. (B) Western blot analysis of MMP11 levels using α-FLAG (anti-FLAG tag) and α-MMP11 (anti-MMP11) antibodies normalized to β-actin to check the overexpression of WT-MMP11 (WT) and Pro78Ser-MMP11 (P78S) in HEK293T cells, compared to empty vector (EV)-transfected controls. (C) Western blot analysis of MMP11 using α-FLAG (anti-FLAG tag) and α-MMP11 (anti-MMP11) antibodies normalized to β-actin to check the overexpression of WT-MMP11 (WT) and MMP11-P78S (P78S) in HCT116 cells, compared to untransfected (UT) or empty vector (EV)-transfected controls. (D) Western blot analysis of MMP11 or FLAG in anti-FLAG immunoprecipitates (IP) to detect the FLAG-pro-MMP11 form showing no signal in cells transfected with the empty vector (EV)-transfected controls. (E) MMP11 activity in immunoprecipitates. Western blot analysis of collagen I in pro-MMP11 WT vs pro-MMP11-P78S immunoprecipitated proteins (l.e, long exposure; s.e, short exposure). (F) MMP11 activity in immunoprecipitates. Western blot analysis of collagen IV in pro-MMP11 WT vs pro-MMP11-P78S immunoprecipitated proteins. (G,H) Invasion of HCT116 cells (transfected as indicated) through collagen (G) or Matrigel (H). The histograms show the mean value ±SEM of the number of invading cells as a fold increase of control (EV) cells (*left*). Representative images of invading cells are also included (*right*). Scale bar = 100 μm. (I) Viability of HCT116 cells (transfected as indicated) at 24 h. The histogram represents the mean value ±SEM of the number of cells as a fold increase of control (EV) cells (*left*). Representative images are also included (*right*). Scale bar = 100 μm

activity assays generating convincing evidence that this variant alters the function of the protein. The functional characterization and the evaluation of the biochemical activity of the hypothetical inactive pro-form of this variant in a CRC cellular model further confirmed its over-activation and its involvement in cell invasion and viability. All this suggests that MMP11-P78S could be playing a role in cancer initiation and progression in the carriers, therefore, being involved in the cancer heritability of this family. Needless to say, that does not rule out that other concomitant factors, whether genetic or environmental, could be also contributing to their increased cancer risk.

The missense variant here described is located in the functional prodomain of MMP11, which precedes the pseudosubstrate region that blocks the catalytic center of the enzyme. When the prodomain is proteolyzed, the pseudosubstrate is released, achieving the activation of the protein.[53] Based on this model, the P78S variant should not affect the functionality of the mature protein. However, this domain is important to maintain the nonmature protein in an inactive state.[53] *In silico* tools predicted a potential conformational change of the MMP11-P78S prodomain, which we hypothesize could prevent its association with the pseudosubstrate, contained in the prodomain, and the active center. This change would allow the enzyme to be active even in a nonmature state. The conservation of the pseudosubstrate residues throughout evolution and the co-segregation of the P78S variant with the CRC phenotype in our familial study, strongly suggest that this region of MMP11 could play a key role in CRC onset and progression. Earlier studies performed by Park and colleagues in 1991 already identified this PRCGVPDV region as a "cysteine switch" and established that the residues immediately surrounding the Cys

are very sensitive to mutational changes.[53] The general model proposed by them suggests that the "cysteine switch" is buried in an "inhibitor pocket" that overlaps, although is not identical to, the substrate-binding site. This pocket would be composed of residues conserved among other MMPs, but not related to substrate specificity, and the PRCGVPDV sequence would establish specific interactions with the conserved residues in this pocket. Thus, even though the different MMPs have different substrate specificities, they could still be inhibited by the same peptide. This model also suggests that alterations of these residues will produce variants with a much-increased tendency to undergo spontaneous activation. Our results showed that MMP11 exists as three different forms in the cellular models analyzed. Two of them conserve an intact N-terminal region, which blocks its activity, while the third one has lost the N-terminal pseudosubstrate domain, becoming active. Based on this general model, more than half of the amount of protein present in the cellular models analyzed, after transfection—with either WT or P78S—, is stored in the cell as pro-MMP11 form while the remaining (around 40%) is in the cleaved/active form. *In vitro* results show that the pro-MMP11-P78S enzyme is able to degrade collagen I and IV while no degradation by WT MMP11 was detected. This confirms that pro-MMP11-P78S displays catalytic activity. According to our model, MMP11-P78S is active in all the states, since it does not need to be activated by furin protease. In contrast, only 40% of the WT version is identified as active/cleaved. This hyper-activation could have pathological consequences. Our findings, consistent with previous studies, explain how a mutation in this domain affects the activity of the protein, as explained in the activation model shown in Figure 6.
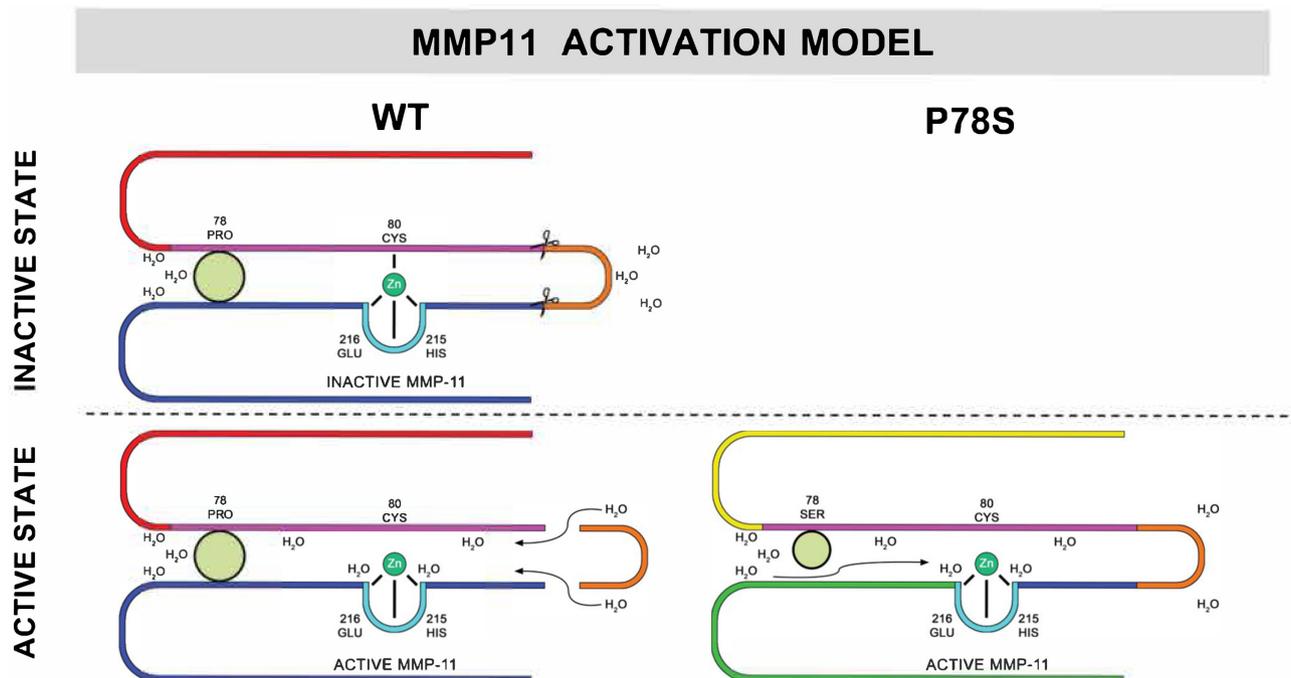
FIGURE 6 MMP11 activation model. MMP11 cysteine switch model of activation described by Ra and Parks (2007) and possible model of MMP11 activation based on the structural data obtained from protein modeling. In this MMP proteolytic activation model, the cleavage causes the access of water, which disrupts the disulfide bond and results in the activation of the enzyme. In the P78S version, due to greater exposure of the pseudosubstrate, proteolytic cleavage is not required for water to gain access and cause the enzyme's activation

These results are also in agreement with accumulating evidence regarding the protumorigenic role of MMP11 and its involvement in cancer development, given that mutations in this region have been associated with a high risk of Uterine Corpus Endometrioid Carcinoma (P78S, COSMIC ID COSM1032603) and lung cancer (R79G, COSMIC ID COSM3309649).[57] However, as previously mentioned, mutations are not the only mechanism by which this gene is able to promote tumorigenic properties. As a matter of fact, *MMP11* expression is found to be upregulated in the serum of cancer patients, as well as in solid tumor tissue samples, while it is almost absent in normal tissues. This upregulation has been identified in a great variety of human cancers, such as oral cancer,[38,58] desmoid tumors,[59] non-small cell lung cancer,[60] esophageal adenocarcinoma,[61] pancreatic adenocarcinoma,[37] aggressive meningioma,[62] colon cancer[39,63,30,40,41] and ovarian carcinoma.[64] Interestingly, *MMP11* upregulation has been found to increase the tumorigenic capacity and metastatic ability of tumor cells in advanced stages.[65] Indeed, our own analysis of TCGA data also showed a strong correlation between *MMP11* expression upregulation and CRC progression, similarly to that observed in previous studies.[40,41] Unfortunately, the mechanism by which MMP11 is overexpressed in CRC (or other tumors) is not completely clear. Some data from previous studies, indicate that histone deacetylases (HDACs) inhibition increased MMP11 expression in colon adenocarcinoma cells.[66] Nonetheless, our in vitro results showed that the overexpression of WT-*MMP11* does not modify the invasive and cell viability properties of the CRC cell line HCT116, while the expression of the P78S version is able to increase them in these already transformed CRC cells. A potential explanation for these results could be that the overexpression by itself is not enough to alter the already enhanced invasive capacity of CRC cells and/or that it is not able to bypass the control mechanisms. This highlights the relevance that the impact of the mutant protein has on these CRC cells, providing these tumorigenic cells with improved invasive, proliferative, survival and metastatic abilities.

In summary and illustrated in a graphical abstract (Figure S3), here we report a variant in the *MMP11* gene, NM_005940: c.232C>T; p.(Pro78Ser), that seems to be implicated in CRC initiation and progression. We hypothesize that this variant could modify the structure of the MMP11 prodomain, producing a premature and/or uncontrolled activation of the enzyme that could contribute to the early CRC onset in these patients. The study of this gene in other familial and sporadic CRC cases will provide further information about its pathogenicity and its role in the heritability of colorectal and other associated cancers, which could contribute to improve the cancer prevention strategies of the carriers in the future.

AUTHOR CONTRIBUTIONS

The work reported in the article has been performed by the authors unless clearly specified in the text. **Lorena Martin-Morales:** Designed the experiments; carried out the experiments and analysis of the data and databases; analyzed the data; wrote the article; provided feedback. **Sara Manzano:** Designed the experiments; carried out the experiments and analysis of the data and databases; analyzed the data; wrote the article; provided feedback. **Maria Rodrigo-Faus:** Designed the experiments; carried out the experiments and analysis of the data and databases; analyzed the data; wrote the article; provided feedback. **Adrian Vicente-Barrueco:** Carried out the experiments and analysis of the data and databases; analyzed the data; provided feedback. **Victor Lorca:** Carried out the experiments and analysis of the data and databases; analyzed the data; provided feedback. **Gonzalo Núñez-Moreno:** Carried out the experiments and analysis of the data and databases; analyzed the data. **Paloma Bragado:** Designed the experiments; carried out the experiments and analysis of the data and databases; analyzed the data; wrote the article; provided feedback. **Almudena Porras:** Designed the experiments; carried out the experiments and analysis of the data and databases; analyzed the data; provided feedback. **Trinidad Caldes:** Designed the experiments; carried out the experiments and analysis of the data and databases; analyzed the data; provided feedback. **Pilar Garre:** Designed the experiments; carried out the experiments and analysis of the data and databases; analyzed the data; provided feedback. **Alvaro Gutierrez-Uzquiza:** Designed the experiments; carried out the experiments and analysis of the data and databases; analyzed the data; wrote the article; provided feedback. All authors read and approved the article.

FUNDING INFORMATION

CONFLICT OF INTEREST

The authors declare no conflicts of interest.

DATA AVAILABILITY STATEMENT

TCGA and CANCERTOOL data: Data is openly available in a public repository. Experimental data: Data available on request from the authors. The raw WES data is available at EGA EGAS00001006489. Other data that support the findings of our study are available from the corresponding author upon request.

ETHICS STATEMENT

The study was approved by the Institutional Review Board of Hospital Clínico San Carlos. A written informed consent was signed by each participant.

ORCID

Lorena Martin-Morales https://orcid.org/0000-0002-1970-8872
Sara Manzano https://orcid.org/0000-0002-0052-511X
Maria Rodrigo-Faus https://orcid.org/0000-0003-1921-6410
Paloma Bragado https://orcid.org/0000-0002-7642-1245
Almudena Porras https://orcid.org/0000-0002-6495-3308
Trinidad Caldes https://orcid.org/0000-0002-1038-5392

Pilar Garre https://orcid.org/0000-0001-8285-4138

Alvaro Gutierrez-Uzquiza https://orcid.org/0000-0002-0446-4131

REFERENCES

1. Grady WM. Genetic testing for high-risk colon cancer patients. *Gastroenterology*. 2003;124:1574-1594.
2. Stoffel EM, Kastrinos F. Familial colorectal cancer, beyond Lynch syndrome. *Clin Gastroenterol Hepatol*. 2014;12:1059-1068.
3. Vasen HF, Mecklin JP, Khan PM, Lynch HT. The international collaborative group on hereditary non-polyposis colorectal cancer (ICG-HNPCC). *Dis Colon Rectum*. 1991;34:424-425.
4. Vasen HF, Watson P, Mecklin JP, Lynch HT. New clinical criteria for hereditary nonpolyposis colorectal cancer (HNPCC, Lynch syndrome) proposed by the international collaborative group on HNPCC. *Gastroenterology*. 1999;116:1453-1456.
5. Lindor NM. Familial colorectal cancer type X: the other half of hereditary nonpolyposis colon cancer syndrome. *Surg Oncol Clin N Am*. 2009;18:637-645.
6. Valle L. Recent discoveries in the genetics of familial colorectal cancer and polyposis. *Clin Gastroenterol Hepatol*. 2017;15:809-819.
7. Zetner DB, Bisgaard ML. Familial colorectal cancer type X. *Curr Genomics*. 2017;18:341-359.
8. Springman EB, Angleton EL, Birkedal-Hansen H, Van Wart HE. Multiple modes of activation of latent human fibroblast collagenase: evidence for the role of a Cys73 active-site zinc complex in latency and a "cysteine switch" mechanism for activation. *Proc Natl Acad Sci U S A*. 1990;87:364-368.
9. Jablonska-Trypuc A, Matejczyk M, Rosochacki S. Matrix metalloproteinases (MMPs), the main extracellular matrix (ECM) enzymes in collagen degradation, as a target for anticancer drugs. *J Enzyme Inhib Med Chem*. 2016;31:177-183.
10. Woessner JF Jr. Matrix metalloproteinases and their inhibitors in connective tissue remodeling. *FASEB J*. 1991;5:2145-2154.
11. Klein T, Bischoff R. Physiology and pathophysiology of matrix metalloproteases. *Amino Acids*. 2011;41:271-290.
12. Nagase H, Visse R, Murphy G. Structure and function of matrix metalloproteinases and TIMPs. *Cardiovasc Res*. 2006;69:562-573.
13. Burrage PS, Mix KS, Brinckerhoff CE. Matrix metalloproteinases: role in arthritis. *Front Biosci*. 2006;11:529-543.
14. Vafadari B, Salamian A, Kaczmarek L. MMP-9 in translation: from molecule to brain physiology, pathology, and therapy. *J Neurochem*. 2016;139(Suppl 2):91-114.
15. Craig VJ, Zhang L, Hagood JS, Owen CA. Matrix metalloproteinases as therapeutic targets for idiopathic pulmonary fibrosis. *Am J Respir Cell Mol Biol*. 2015;53:585-600.
16. DeLeon-Pennell KY, Meschiari CA, Jung M, Lindsey ML. Matrix metalloproteinases in myocardial infarction and heart failure. *Prog Mol Biol Transl Sci*. 2017;147:75-100.
17. Itoh Y, Nagase H. Matrix metalloproteinases in cancer. *Essays Biochem*. 2002;38:21-36.
18. Quintero-Fabian S, Arreola R, Becerril-Villanueva E, et al. Role of matrix Metalloproteinases in angiogenesis and cancer. *Front Oncol*. 2019;9:1370.
19. Gonzalez-Avila G, Sommer B, Mendoza-Posada DA, Ramos C, Garcia-Hernandez AA, Falfan-Valencia R. Matrix metalloproteinases participation in the metastatic process and their diagnostic and therapeutic applications in cancer. *Crit Rev Oncol Hematol*. 2019;137:57-83.
20. Limb GA, Matter K, Murphy G, et al. Matrix metalloproteinase-1 associates with intracellular organelles and confers resistance to lamin A/C degradation during apoptosis. *Am J Pathol*. 2005;166:1555-1563.
21. Kwan JA, Schulze CJ, Wang W, et al. Matrix metalloproteinase-2 (MMP-2) is present in the nucleus of cardiac myocytes and is capable of cleaving poly (ADP-ribose) polymerase (PARP) in vitro. *FASEB J*. 2004;18:690-692.
22. Pei D, Weiss SJ. Furin-dependent intracellular activation of the human stromelysin-3 zymogen. *Nature*. 1995;375:244-247.
23. Luo D, Mari B, Stoll I, Angland P. Alternative splicing and promoter usage generates an intracellular stromelysin 3 isoform directly translated as an active matrix metalloproteinase. *J Biol Chem*. 2002;277:25527-25536.
24. Ra HJ, Parks WC. Control of matrix metalloproteinase catalytic activity. *Matrix Biol*. 2007;26:587-596.
25. Bassi DE, Mahloogi H, Klein-Szanto AJ. The proprotein convertases furin and PACE4 play a significant role in tumor progression. *Mol Carcinog*. 2000;28:63-69.
26. Sun Y, Vandenbriele C, Kauskot A, Verhamme P, Hoylaerts MF, Wright GJ. A human platelet receptor protein microarray identifies the high affinity immunoglobulin E receptor subunit alpha (FcepsilonR1alpha) as an activating platelet endothelium aggregation receptor 1 (PEAR1) ligand. *Mol Cell Proteomics*. 2015;14:1265-1274.
27. Pei D, Majmudar G, Weiss SJ. Hydrolytic inactivation of a breast carcinoma cell-derived serpin by human stromelysin-3. *J Biol Chem*. 1994;269:25849-25855.
28. Manes S, Mira E, Barbacid MM, et al. Identification of insulin-like growth factor-binding protein-1 as a potential physiological substrate for human stromelysin-3. *J Biol Chem*. 1997;272:25706-25712.
29. Pan W, Arnone M, Kendall M, et al. Identification of peptide substrates for human MMP-11 (stromelysin-3) using phage display. *J Biol Chem*. 2003;278:27820-27827.
30. Peruzzi D, Mori F, Conforti A, et al. MMP11: a novel target antigen for cancer immunotherapy. *Clin Cancer Res*. 2009;15:4104-4113.
31. Yang H, Jiang P, Liu D, et al. Matrix metalloproteinase 11 is a potential therapeutic target in lung adenocarcinoma. *Mol Ther Oncolytics*. 2019;14:82-93.
32. Duan S, Guo Y. Expression and clinical significance of stromelysin-3 in laryngeal cancer. *Lin Chung Er Bi Yan Hou Tou Jing Wai Ke Za Zhi*. 2008;22:104-107.
33. Thorns V, Walter GF, Thorns C. Expression of MMP-2, MMP-7, MMP-9, MMP-10 and MMP-11 in human astrocytic and oligodendroglial gliomas. *Anticancer Res*. 2003;23:3937-3944.
34. Xu G, Zhang B, Ye J, et al. Exosomal miRNA-139 in cancer-associated fibroblasts inhibits gastric cancer progression by repressing MMP11 expression. *Int J Biol Sci*. 2019;15:2320-2329.
35. Wang Y, Wei Y, Fan X, et al. MicroRNA-125b as a tumor suppressor by targeting MMP11 in breast cancer. *Thorac Cancer*. 2020;11:1613-1620.
36. Han J, Choi YL, Kim H, et al. MMP11 and CD2 as novel prognostic factors in hormone receptor-negative, HER2-positive breast cancer. *Breast Cancer Res Treat*. 2017;164:41-56.
37. von Marschall Z, Riecken EO, Rosewicz S. Stromelysin 3 is overexpressed in human pancreatic carcinoma and regulated by retinoic acid in pancreatic carcinoma cell lines. *Gut*. 1998;43:692-698.
38. Soni S, Mathur M, Shukla NK, Deo SV, Ralhan R. Stromelysin-3 expression is an early event in human oral tumorigenesis. *Int J Cancer*. 2003;107:309-316.
39. Skoglund J, Emterling A, Arbman G, Angland P, Sun XF. Clinicopathological significance of stromelysin-3 expression in colorectal cancer. *Oncology*. 2004;67:67-72.
40. Eiro N, Carrion JF, Cid S, et al. Toll-like receptor 4 and matrix metalloproteases 11 and 13 as predictors of tumor recurrence and survival in stage II colorectal cancer. *Pathol Oncol Res*. 2019;25:1589-1597.
41. Tian X, Ye C, Yang Y, et al. Expression of CD147 and matrix metalloproteinase-11 in colorectal cancer and their relationship to clinicopathological features. *J Transl Med*. 2015;13:337.
42. Yang YH, Deng H, Li WM, et al. Identification of matrix metalloproteinase 11 as a predictive tumor marker in serum based on gene expression profiling. *Clin Cancer Res*. 2008;14:74-81.

43. Zhou N, Gutierrez-Uzquiza A, Zheng XY, et al. RUNX proteins desensitize multiple myeloma to lenalidomide via protecting IKZFs from degradation. *Leukemia*. 2019;33:2006-2021.

44. Inanc S, Keles D, Oktay G. An improved collagen zymography approach for evaluating the collagenases MMP-1, MMP-8, and MMP-13. *Biotechniques*. 2017;63:174-180.

45. Yang J, Yan R, Roy A, Xu D, Poisson J, Zhang Y. The I-TASSER suite: protein structure and function prediction. *Nat Methods*. 2015;12:7-8.

46. Roy A, Kucukural A, Zhang Y. I-TASSER: a unified platform for automated protein structure and function prediction. *Nat Protoc*. 2010;5:725-738.

47. Zhang Y. I-TASSER server for protein 3D structure prediction. *BMC Bioinform*. 2008;9:40.

48. Zhang Y, Skolnick J. TM-align: a protein structure alignment algorithm based on the TM-score. *Nucleic Acids Res*. 2005;33:2302-2309.

49. Moretti S, Armougom F, Wallace IM, Higgins DG, Jongeneel CV, Notredame C. The M-coffee web server: a meta-method for computing multiple sequence alignments by combining alternative alignment methods. *Nucleic Acids Res*. 2007;35:W645-W648.

50. Wallace IM, O'Sullivan O, Higgins DG, Notredame C. M-coffee: combining multiple sequence alignment methods with T-coffee. *Nucleic Acids Res*. 2006;34:1692-1699.

51. Robert X, Gouet P. Deciphering key features in protein structures with the new ENDscript server. *Nucleic Acids Res*. 2014;42:W320-W324.

52. Cortazar AR, Torrano V, Martin-Martin N, et al. CANCERTOOL: a visualization and representation interface to exploit cancer datasets. *Cancer Res*. 2018;78:6320-6328.

53. Park AJ, Matrisian LM, Kells AF, Pearson R, Yuan ZY, Navre M. Mutational analysis of the transin (rat stromelysin) autoinhibitor region demonstrates a role for residues surrounding the "cysteine switch". *J Biol Chem*. 1991;266:1584-1590.

54. Egeblad M, Werb Z. New functions for the matrix metalloproteinases in cancer progression. *Nat Rev Cancer*. 2002;2:161-174.

55. Herszenyi L, Hritz I, Lakatos G, Varga MZ, Tulassay Z. The behavior of matrix metalloproteinases and their inhibitors in colorectal cancer. *Int J Mol Sci*. 2012;13:13240-13263.

56. Nejadtaghi M, Jafari H, Farrokhi E, Samani KG. Familial colorectal cancer type X (FCCTX) and the correlation with various genes: a systematic review. *Curr Probl Cancer*. 2017;41:388-397.

57. McMillan EA, Ryu MJ, Diep CH, et al. Chemistry-first approach for nomination of personalized treatment in lung cancer. *Cell*. 2018;173:864-878.

58. Arora S, Kaur J, Sharma C, et al. Stromelysin 3, Ets-1, and vascular endothelial growth factor expression in oral precancerous and cancerous lesions: correlation with microvessel density, progression, and prognosis. *Clin Cancer Res*. 2005;11:2272-2284.

59. Denys H, De Wever O, Nusgens B, et al. Invasion and MMP expression profile in desmoid tumours. *Br J Cancer*. 2004;90:1443-1449.

60. Kettunen E, Anttila S, Seppanen JK, et al. Differentially expressed genes in nonsmall cell lung cancer: expression profiling of cancer-related genes in squamous cell lung cancer. *Cancer Genet Cytogenet*. 2004;149:98-106.

61. Hourihan RN, O'Sullivan GC, Morgan JG. Transcriptional gene expression profiles of oesophageal adenocarcinoma and normal oesophageal tissues. *Anticancer Res*. 2003;23:161-165.

62. Perret AG, Duthel R, Fotso MJ, Brunon J, Mosnier JF. Stromelysin-3 is expressed by aggressive meningiomas. *Cancer*. 2002;94:765-772.

63. Han HB, Gu J, Zuo HJ, et al. Let-7c functions as a metastasis suppressor by targeting MMP11 and PBX3 in colorectal cancer. *J Pathol*. 2012;226:544-555.

64. Mueller J, Brebeck B, Schmalfeldt B, Kuhn W, Graeff H, Hofler H. Stromelysin-3 expression in invasive ovarian carcinomas and tumours of low malignant potential. *Virchows Arch*. 2000;437:618-624.

65. Andarawewa KL, Boulay A, Masson R, et al. Dual stromelysin-3 function during natural mouse mammary tumor virus-ras tumor progression. *Cancer Res*. 2003;63:5844-5849.

66. Barrasa JI, Olmo N, Santiago-Gomez A, et al. Histone deacetylase inhibitors upregulate MMP11 gene expression through Sp1/Smad complexes in human colon adenocarcinoma cells. *Biochim Biophys Acta*. 1823;2012:570-581.

SUPPORTING INFORMATION

Additional supporting information can be found online in the Supporting Information section at the end of this article.